*Int. J. Multiphase Flow* Vol. 17, No. 5, pp. 585–598, 1991
Printed in Great Britain. 
0301-9322/91 $3.00 + 0.00


# A COMBINED LASER DOPPLER ANEMOMETRY AND ELECTRICAL PROBE DIAGNOSTIC FOR BUBBLY TWO-PHASE FLOW

Y. Y. SHENG and G. A. IRONS
Department of Materials Science and Engineering, McMaster University, Hamilton, Ontario, Canada

*(Received 1 February 1990; in revised form 1 May 1991)*

**Abstract**—A review of the literature on laser Doppler anemometry (LDA) techniques to discriminate liquid from bubble velocities reveals that the techniques are unsuitable for large bubbles at moderate void fractions. A statistical technique, based on the separation of the combined gas and liquid velocity distribution function, was investigated. It was found to be appropriate for uniformly sized bubbles, a condition which is most easily achieved with small bubbles (< 4 mm dia). A combined LDA and electrical probe (EP) technique was also developed to simultaneously measure the velocities from both the liquid and gaseous phase in unconfined two-phase bubbly plumes. The simultaneous time series of LDA velocities and EP signals from a chain of bubbles permitted separation of gas and liquid velocities at high volume fractions and for large, irregular bubbles.

*Key Words:* laser Doppler anemometer, electric probe, bubble velocity, multi-phase, fluid flow, velocity separation

## INTRODUCTION

Unconfined, bubbly, gas–liquid plumes are of general interest in several fields of engineering: chemical engineering reactor design; the destratification of lake water; and in metallurgical reactor design. The situation in liquid metal reactor vessels is somewhat different from aqueous systems; the bubbles tend to be larger (> 10 mm dia) because bubbles spread across injection orifices due to poor wetting of the orifice (Irons & Guthrie 1981), and because the bubbling regime extends to higher injection velocities before jetting occurs (Zhao & Irons 1989). In some processes, only low gas velocities are employed (for non-metallic inclusion flotation or thermal homogenization), in which case the void fractions in the plume are of the order of 0.05–0.10. To carry out chemical reactions, such as steel or copper making, the injection velocities are much higher and the corresponding void fractions will be much higher.

On the basis of Morton number similarity, gas injection into water is often used as a convenient, transparent analog for injection into liquid metals. To artificially increase bubble volumes in aqueous systems to make them comparable to metallic systems, the capacitance of the gas train can be increased (Irons & Guthrie 1981).

In order to study transport phenomena between the gas and liquid, the velocities of each phase must be measured. The following review of the literature shows that most of the previous techniques to measure gas and liquid velocities using laser Doppler anemometry (LDA) are best-suited to small bubbles at low volume fraction. This deficiency led to the development of the present technique.

## REVIEW OF THE LITERATURE

### *LDA for two-phase flow diagnostics*

LDA has become the pre-eminent technique for velocity measurement in transparent single-phase flow. Seeding particles, which scatter the laser light, are smaller than the control volume (Drain 1980), and generally follow the flow. Larger particles and bubbles will also scatter light, therefore special equipment and procedures are necessary to distinguish the signals from the seeds in the continuous phase and those from the other phases. There has been considerable work in this field to measure bubble or particle velocity, bubble diameter, frequency and void fraction. The equipment required, and discrimination techniques are summarized in table 1. The techniques fall into three main categories.

*Discrimination based on the signal wave form.* Durst & Zare (1975) were the first to analyze the amplitude and frequency of the Doppler signal in several two-phase systems. Boerner *et al.* (1984) extended the technique to eliminate signals from the bubbles. Lee and coworkers (Lee & Srinivasan 1978; Lee & Durst 1982; Lee & Cho 1983) used signal amplitude gating together with time or frequency discrimination with specially designed filterbanks. Martin *et al.* (1981) found that bubble size and Doppler pedestal amplitude are linearly related, so that an adjustable pinhole aperture was developed to measure the bubble size and velocity. The techniques employed by Tsuji and coworkers (Tsuji & Morikawa 1982; Tsuji *et al.* 1984) and Ueda *et al.* (1986) are also in this first category.

*Discrimination based on signal analysis and light blocking.* These techniques use photodiodes which monitor when the laser beam is interrupted by a bubble along the path of the beam. For discrimination of bubble velocity this technique is limited to low void fractions, where one is certain that only bubbles in the control volume interrupt the beam. The technique was used by Lee & Srinivasan (1982), Lee & Cho (1983) and Ohba *et al.* (1986). Ohba *et al.* (1976a,b) also used photodiodes to measure light attenuation through bubbly flow to obtain the line-average void fraction. Durst *et al.* (1986) used a much more complicated set-up with two LDAs, two

Table 1. LDA for the two-phase flow measurement

| Reference | Laser and optics | Data taken | Data analyzer | Discrimination technique |
|---|---|---|---|---|
| Boerner *et al.* (1984) | 15 mW He–Ne | $U_L$ | Counter | Amplitude analysis |
| Durst & Zare (1975) | 15 mW He–Ne 2 PMT or 2 PD | $U_p$ $U_b$ | Multichannel analyzer | Signal characteristic analysis (amplitude and wave shape) |
| Durst *et al.* (1986) | 2 LDA 15 mW He–Ne 2 PMT 4 PD | $U_b$, $U_L$ $U_b$, $f_b$ | Frequency tracker | Amplitude and blockage of light to photodiodes |
| Lee & Srinivasan (1978) | 15 mW He–Ne | PDF of $U_p$ | Tracker and counter | Amplitude and time discrimination |
| Lee & Durst (1982) | 15 mW 1 PMT 2 PD | $U_p$ $U_G$ | Unknown | Amplitude and frequency discrimination with special filterbanks |
| Lee & Srinivasan (1982) | 15 mW He–Ne 1 PMT 1 PD | $U_p$ $U_p$ | Counter | Amplitude gating and light blocking |
| Lee & Cho (1983) | 15 mW He–Ne 2PMT 1 PD | $U_p$ $D_p$ | Two counters | Amplitude gating and light blocking |
| Marie & Lance (1983) | Unknown | $U_b$ $U_L$ | Frequency tracker | Two distinct peaks on the velocity PDF |
| Martin *et al.* (1981) | 5 mW He–Ne 2 PMT | $U_b$ $D_b$ | Unknown | Pinhole aperture for amplitude analysis |
| Momii *et al.* (1986) | Unknown | $U_L$ $U_p$ | Unknown | Forward scattering for $U_L$ backward for $U_p$ |
| Ohba *et al.* (1976a,b) | 15 mW He–Ne | $U_L$ $\varepsilon$ | Spectrum analyzer etc. | Light attenuation for void fraction |
| Ohba *et al.* (1986) | 15 mW He–Ne 2 PMT | $U_L$ $U_b$ | Spectrum analyzer etc. | Light blocking of one PMT for $U_b$ |
| Tsuji & Morikawa (1982) Tsuji *et al.* (1984) | 15 mW He–Ne | $U_p$ $U_G$ | Tracker and special signal analyzer | Amplitude analyzer of both the Doppler signal and the pedestals |
| Ueda *et al.* (1986) | Unknown | $U_L$ $U_p$ | Unknown | Setting the optimum threshold values for the Doppler signal amplitude |

photomultiplier tubes and four photodiodes to measure liquid and bubble velocities, bubble size and bubble frequency (amplitude discrimination was also utilized). Momii *et al.* (1986) measured the liquid velocity from the forward-scattered radiation and the particle velocity from back-scattered signals: however, it is not certain that liquid signals were excluded from the back-scattered signals.

*Discrimination based on the velocity distribution.* Marie & Lance (1983) found that the velocity probability distribution function at low void fraction flow has two distinct peaks representing liquid and bubble velocities, respectively.

*Electrical probe (EP) measurements for bubbly two-phase flows*

Electrical or impedance probes have long been used to measure void fractions in two-phase flow; for reviews, see Hinze (1975) and Banerjee & Lahey (1981). More sophisticated probes have also been used to measure bubble velocity and liquid velocity. Recently, Hardy & Hylton (1984) used double-probes or string-probes to measure the bubble and liquid velocities. Serizawa *et al.* (1975a–c) also used the double-probe technique to perform extensive measurements of bubbly two-phase flow inside a pipe; they systematically measured bubble frequency, void fraction distribution and bubble velocity. More recently, Castillejos & Brimacombe (1987a,b) used a specially designed double-EP system to measure the spatial distributions of bubble frequency, void fraction and bubble rising velocity inside a bubbly plume.

*General comments*

The first two LDA techniques both require extra equipment and complicated data processing. All three LDA techniques have only been applied in limited circumstances, i.e. in a low volume fraction chain of small bubbles with fairly smooth interfaces or in a particulate two-phase flow where signals from the two phases are quite different from each other. There are three major problems in making measurements with larger bubbles at high void fractions:

(1) Due to the distorted shapes and wobbling interfaces of large bubbles, the signals from the bubbles are not always stronger than those from the liquid. This makes amplitude discrimination techniques difficult. Another shortcoming of the amplitude discrimination technique is that the measuring time is very long, in some instances $>30$ min to measure the velocity at one point inside a chain of bubbles (Boerner *et al.* 1984).
(2) Since there are many bubbles present at the same time inside the bubbly plume, it is not certain that the interruption of light to the photomultiplier tube (PMT) or photodiode was caused by the bubble at the focus. Thus, the focus may be in the liquid, and generate a Doppler signal to the PMT, while the photodiode is interrupted by a bubble not at the focus. This data would be incorrectly attributed to a bubble. This makes the light-blocking techniques difficult.
(3) There is considerable overlap in the velocity probability distribution functions for the gas and the liquid. This makes techniques based on inspection of the distributions difficult.

In this paper, techniques involving the manipulation of the velocity distributions were investigated, and found to be of limited value for large bubbles. Therefore, a new technique, which takes advantage of both the LDA and the EP techniques using only one laser, one PMT, one counter and a single-tip EP has been developed to measure bubble and liquid velocities, void fraction and bubble frequency inside plumes with large fractions of big bubbles.

## APPARATUS

Two vessels were used for the investigations. A small plexiglass box ($100 \times 100$ mm$^2$ $\times$ 150 mm high) was used at low flow rates in which individual bubbles followed each other in single file without touching each other (bubble chains). The box was filled with distilled water to 125 mm in depth. A 4 mm i.d. copper tube was placed 25 mm above the bottom.

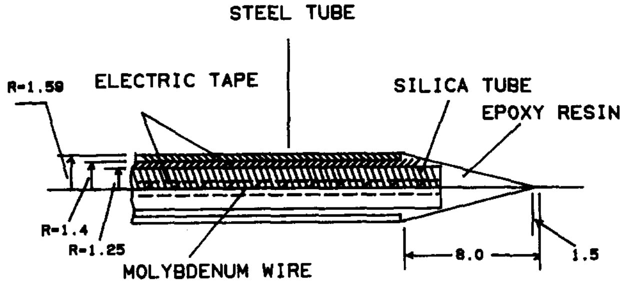


Figure 1. Details of the EP tip.

The other vessel was a 1/10 scale model of a steelmaking ladle. Higher flow rates were used in this vessel. The model consisted of a 500 mm dia cylinder 760 mm high, inside an outer box $560 \times 560 \text{ mm}^2 \times 760$ mm high. Both the cylinder and the outer box were filled with distilled water to minimize distortion due to curvature of the inner cylinder. Five horizontal slots were cut on the inner cylinder wall to eliminate the curvature effect for lateral velocity measurements; the slots were 3 mm high and one-quarter of the cylinder circumference long. Two types of injectors were used. A glass lance with fritted glass at the end was used to produce small bubbles, 0.5–4 mm dia. Larger bubbles (approx. 5–40 mm dia) were produced by a flush-mounted orifice (4 mm dia) located at the centre of the bottom.

The LDA used in this work was DANTEC Model 127 (He–Ne) with a power of 60 mW which could be used both for forward and backward scattering. The focal lengths of the objective lenses were 80 and 310 mm.

A DISA 55L90a counter was used to process the LDA data. Two operational modes were used: Fixed and Combined. Under the Fixed mode operation, data are taken whenever a signal is validated, while only one datum is taken from one signal burst in the Combined mode. There are also two modes for the LDA interface to the computer: Timer and LDA. In the Timer mode, data are taken at a pre-determined time interval; however in the LDA mode, the Data Ready command is enabled by a validated signal itself, thus data is taken as rapidly as possible (cf. Tropea & Struthers 1987).

The construction of the EP tip used in this experiment is shown in figure 1. To increase sensitivity, the bridge circuit shown in figure 2 was developed. The EP signals were collected by the same A/D interface as the LDA signals, thus it operated in either the Timer or LDA mode described above. The data acquisition rate could be varied between 80 and 140 kHz. The EP was bent into a "dog-leg" shape so that the tip could be positioned $<1$ mm below the LDA focus without interrupting the beam.

## EXPERIMENTAL RESULTS

### *Evaluation of the combined LDA/EP technique*

For preliminary evaluation of the combined LDA/EP technique, chains of bubbles were generated in the small plexiglass box. The EP was positioned 45 mm above the nozzle. The gas flow

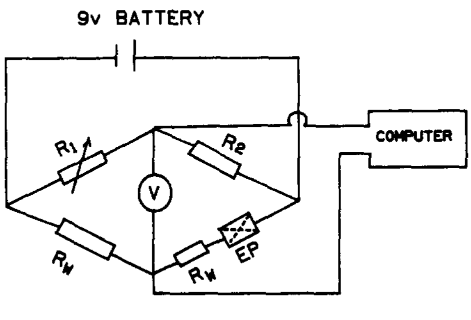


Figure 2. EP circuit to improve sensitivity.

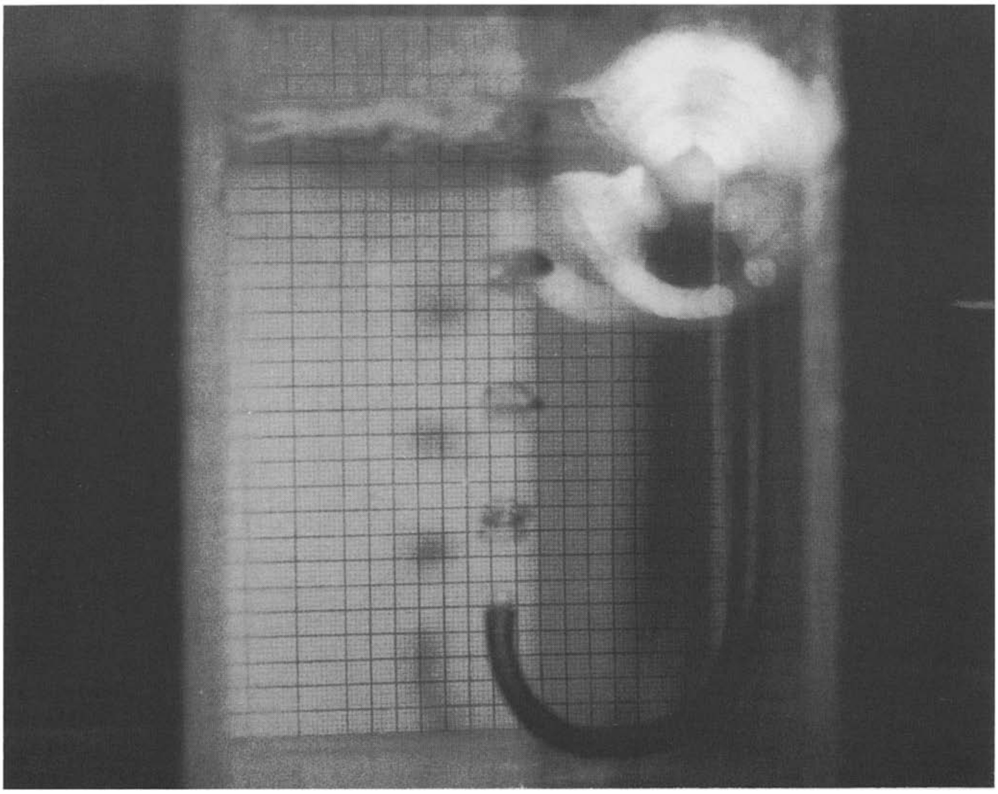

Figure 3. Photograph of bubble chain in the small tank. The bright spot at the upper right corner is the reflection of the strobe light. The injector used has i.d. = 4 mm and o.d. = 6 mm. The strobe light frequency was 105 Hz, the gas flowrate ($Q_G$) was $5 \times 10^{-6}$ $Nm^3/s$, $U_b = 0.40$ m/s, $\epsilon = 0.31$, $f_b = 14.5$ s and $D_b = 8.8$ mm.

rate was varied between 0.58 and 20.2 ml/s. In order to improve the liquid velocity signals, small quantities of market rice powder were used for seeding. With proper seeding, acceptable data rates could be achieved (0.1–0.2 kHz).

To calibrate the combined LDA/EP technique for bubble frequency, void fraction and bubble velocity, still photographs were taken with strobelight illumination. The movement of bubbles during the time interval between two flashes is shown in figure 3. The simultaneous variation of the EP voltage and LDA velocity with time are shown in figures 4 and 5, for forward and backward

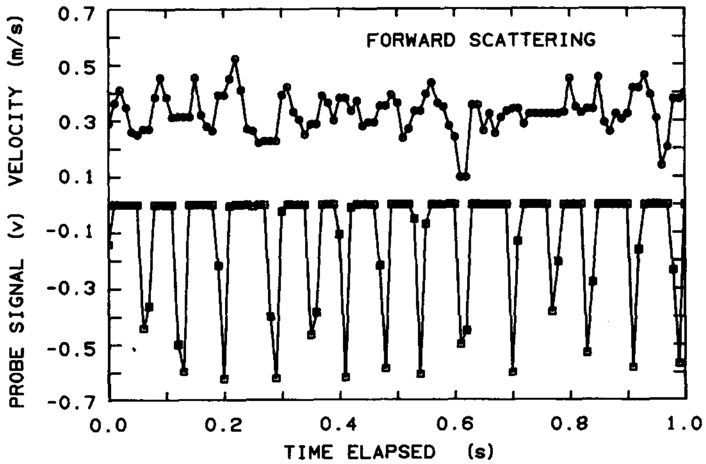


Figure 4. Time series of velocity (upper) and EP voltage (lower) produced in the forward-scattering configuration. This was performed in the small box with a 4 mm dia nozzle. The LDA was operated under the Fixed/Timer mode. $Q_G = 5.0 \times 10^{-6}$ $Nm^3/s$, $U_b = 0.40$ m/s, $\epsilon = 0.31$, $f_b = 14.5$ s and $D_b = 8.8$ mm.

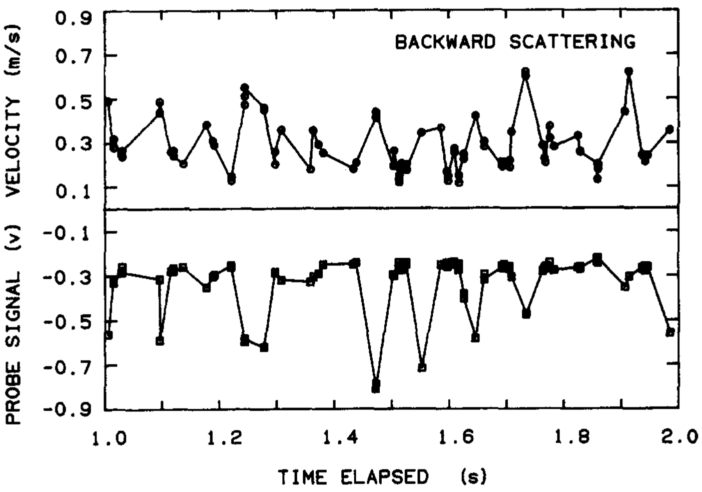


Figure 5. Time series of velocity (upper) and EP voltage (lower) produced in the backward-scattering configuration. This experiment was performed in the small box with the 4 mm dia nozzle. The LDA was operated under the Combined/LDA mode. $Q_G = 7.75 \times 10^{-6}$ Nm$^3$/s, $U_b = 0.44$ m/s, $\epsilon = 0.38, f_b = 15$ s and $D_b = 9.96$ mm.

scattering, respectively. In figure 4, the LDA was operating under the Timer mode, so that both LDA and EP data were obtained at a pre-set frequency of 0.1 kHz. The EP voltage data are straightforward, however, the LDA velocity data are not. At the time when data was to be taken, if there were a validated velocity datum, then this datum was recorded as a true value. If there were none, then the previous velocity datum would be taken as the present value. Furthermore, forward scattering was used, therefore most bubble velocity data could not be recorded because of the blockage to the PMT by the bubble at the focus. On the other hand, in figure 5, the LDA was working under the LDA mode (enabled by valid LDA signals) and backward scattering was used. The velocity variation caused by bubble passage was well-recorded and indicated by the EP voltage response. Even without the information from the EP on the presence of bubbles, the liquid and gas velocities can be clearly distinguished when there is only a low frequency chain of bubbles.

When bubble velocities are separated from the liquid velocities on the basis of the probe measurement, they compare favourably with those measured from the strobe photographs as

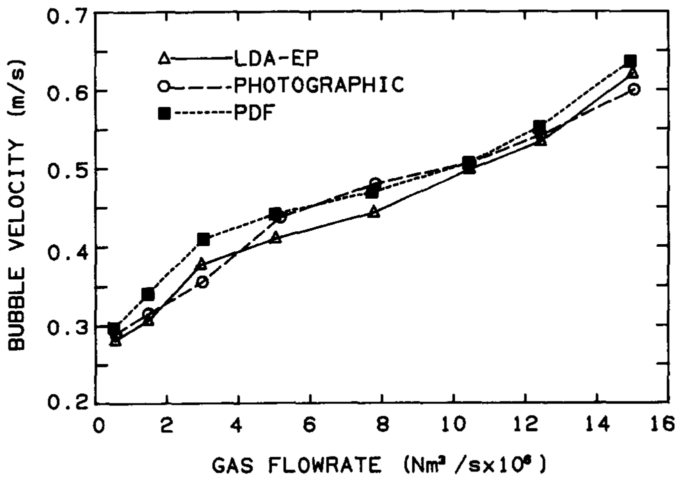


Figure 6. Bubble velocity measured by three different methods in a bubble chain. In the photographic technique the distance travelled between strobe flashes was used. The LDA/EP technique simply involved inspection of the EP voltage time series for bubble velocities. The PDF technique is described in the text. The agreement between the methods is very good. For these experiments the small box was used with a 4 mm dia nozzle. The LDA was operated under the Combined/LDA mode with backward scattering.

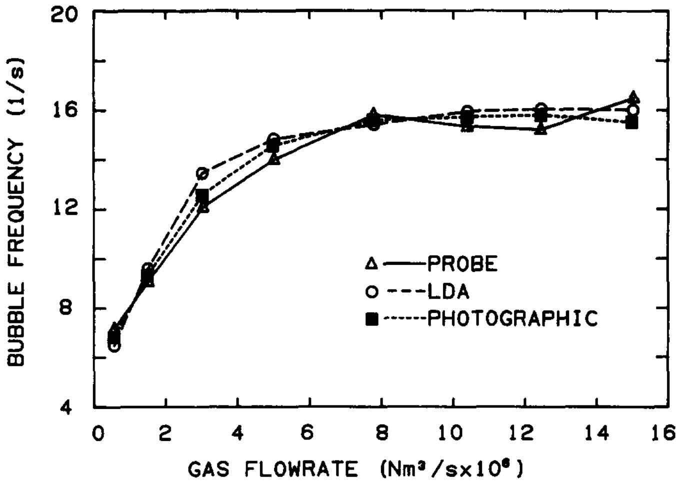


Figure 7. Bubble frequency measured by three different methods in a bubble chain. The LDA method involved inspection of the velocity time series. The photographic technique is described in the text. For these experiments the small box was used with a 4 mm dia nozzle. The LDA was operated under the Combined/LDA mode with backward scattering.

shown in figure 6. The difference between them is negligible at 95% significance level, using Student's $t$-test.

Bubble frequency can be measured by either the EP or by visual inspection of the LDA velocity time series, such as in figures 4 and 5; however, the latter method can only produce good bubble frequency measurements when the void fraction is low and the passage of bubble is clearly indicated by the peak velocity variation. In such situations there is good agreement with frequencies from the strobe photographs; the difference is <5% (figure 7).

The present LDA velocity time series, by itself, cannot be used to obtain the void fraction, because the data rate is too low to produce several signals during the passage of a bubble, thus the time resolution is poor. On the other hand, the electrical probe data are reliable measures of the time-averaged void fraction, as discussed in the Review of the Literature section. The time-averaged void fraction, $\epsilon$, was independently calculated from the bubble size, bubble frequency and bubble velocity which were measured from the photographs:

$$\epsilon = f_b D_{bh}/U_b, \qquad [1]$$

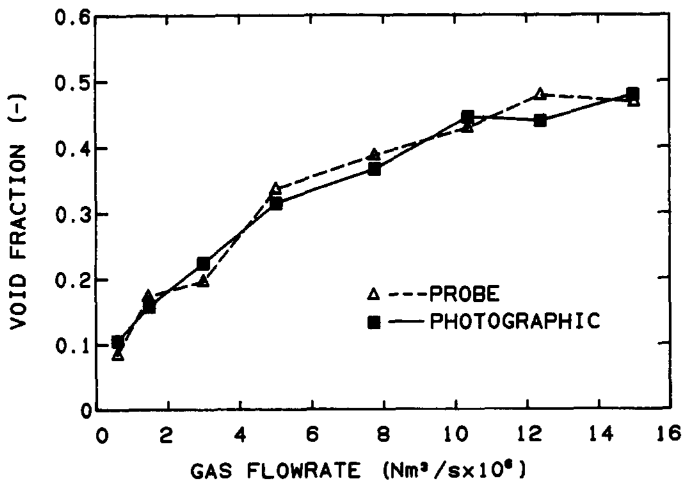


Figure 8. Void fraction measured by the EP and photographic techniques which are described in the text. The bubble chain was produced in a small box (100 × 100 mm² × 150 mm high). For these experiments the small box was used with a 4 mm dia nozzle. The LDA was operated under the Fixed/Timer mode with data acquisition rate of 0.1 Hz for $f_b$ and $\epsilon$.

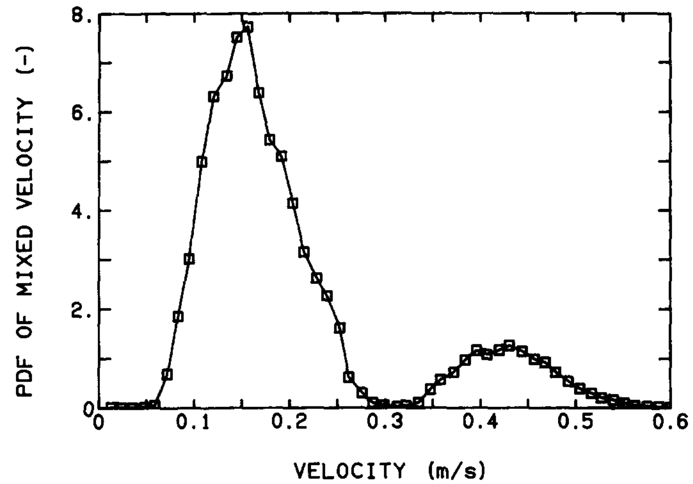


Figure 9. Velocity PDF for the gas and liquid velocities. The plume consisted of small bubbles (approx. 2 mm dia) produced with a fritted glass injector inside the model. The data were taken at a position 30 mm above the injector and 10 mm away from the plume centreline. The LDA was operated under the Combined/LDA mode with backward scattering. $Q_G = 5.0 \times 10^{-6}\ \mathrm{Nm^3/s}$ and $\epsilon$ was estimated to be approx. 0.01 at this position.

where $f_b$ is the bubble frequency, $D_{bh}$ is the bubble height in the rising direction and $U_b$ is the bubble velocity. As figure 8 shows there is good agreement for the void fraction from the photographic and EP techniques; the differences are negligible at the 95% significance level.

## APPLICATIONS

### *Liquid and gas velocities in plumes*

Very small bubbles are produced when gas is injected through the fritted glass, and in these cases it is easy to see the velocity distributions for the gas and liquid because there is little overlap (figure 9). However, for bottom injection the bubbles are considerably bigger and there is more overlap in the probability distribution function (PDF). For example, in figure 10, the bubble velocities appear at the knee at approx. 0.3 m/s, so that visual inspection cannot be used to separate the distributions. A statistical technique was investigated to solve this problem.

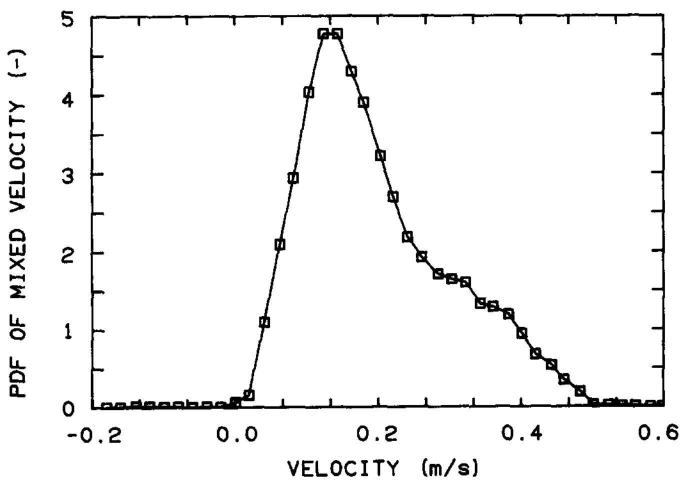


Figure 10. Velocity PDF in a chain of bubbles. The chain was produced in the small box with a 4 mm dia injector. The LDA was operated under the Combined/LDA mode with backward scattering. $Q_G = 1.5 \times 10^{-6}\ \mathrm{Nm^3/s}$, $U_b = 0.32$ m/s, $\epsilon = 0.18$, $f_b = 9.2$ s and $D_b = 6.8$ mm.

*Discrimination by mixture PDF*

The statistical technique is best described graphically. Independent normal distributions of the gas and liquid velocities will appear as straight lines in normal probability plots, as shown in figure 11. Mixtures of these two distributions according to

$$U_m = \epsilon U_G + (1 - \epsilon) U_L \qquad [2]$$

with various void fractions, $\epsilon$, will not be straight except at the tails of the distribution. Tangents to the tails represent the superficial velocity distributions of the gas, $\epsilon U_G$, and liquid, $(1 - \epsilon)U_L$. These relationships were used in the following procedure to separate the gas and liquid velocities:

(1) Plot the mixture velocity distribution on normal probability paper, as illustrated in figures 12 and 13, for the data in figures 9 and 10, respectively.
(2) Construct tangents to the tails to obtain the superficial velocity distributions for gas and liquid, $\epsilon U_G$ and $(1 - \epsilon)U_L$.
(3) Make an initial guess of the void fraction, $\epsilon$.
(4) With knowledge of $\epsilon U_G$ and $(1 - \epsilon)U_L$ at the tails, and the guess of $\epsilon$, the $U_G$ and $U_L$ distributions can be obtained by considering these portions of $U_G$ and $U_L$ as independent distributions and recalculating their PDF.
(5) With these estimates of $\epsilon$, $U_G$ and $U_L$, calculated the $U_m$ of the distribution for this mixture using [2].
(6) Compare the calculated $U_m$ distribution with the actual one, and adjust $\epsilon$ to minimize the sum of squares between the two by looping through steps 4 and 5.
(7) Plot $U_G$ and $U_L$ distributions, along with the raw data, as seen in figures 12 and 13. The mean velocities and RMS values can be immediately determined.

Velocities determined in this way agree very well with those measured from photographs, and with velocity discrimination on the basis of the probe (figure 6). With larger bubbles and higher void fractions it is not possible to separate the two distributions with this technique, this problem led to the development of the combined LDA/EP technique.

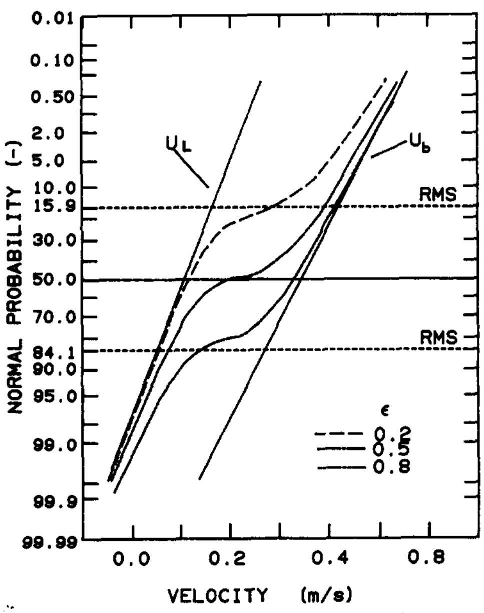


Figure 11. Graphical representation of the combined gas and liquid PDFs. The dotted lines represent the summation of two independent distributions for $U_L$ and $U_b$ for various volume fraction weightings.

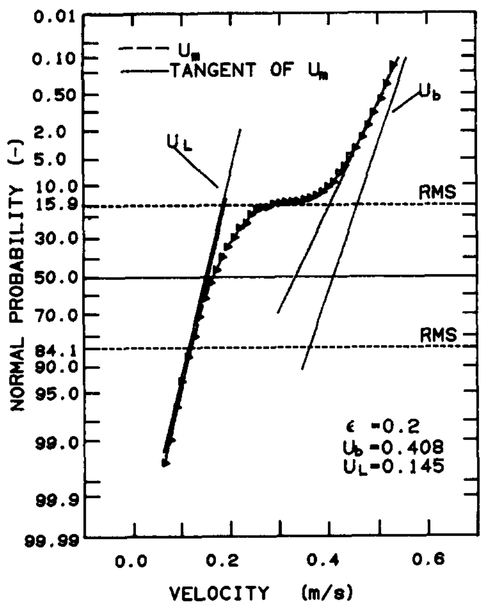


Figure 12. PDF of the mixed velocity for the data in figure 9. The constructions for the tangents (superficial velocity distributions) and gas and liquid velocities are superimposed.

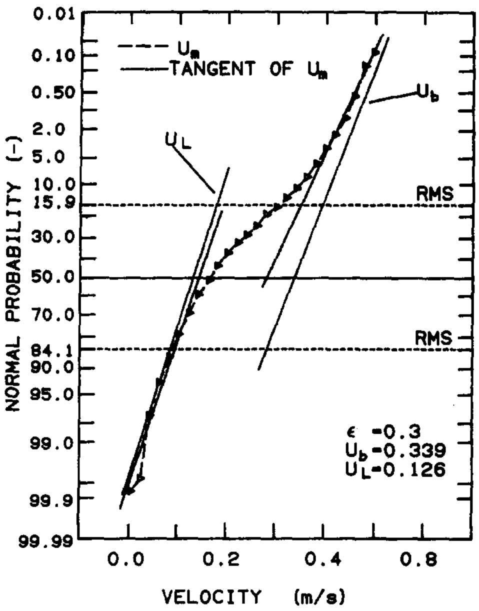


Figure 13. PDF of the mixed velocity for the data in figure 10. The constructions for the tangents (superficial velocity distributions) and gas and liquid velocities are superimposed.

*Discrimination by the combined LDA/EP technique*

Results are presented in figure 14 for the mean and RMS values of gas and liquid velocity for large bubbles (10–40 mm dia) at void fractions of 0.06–0.12. Note that in these plumes the RMS values for gas and liquid are generally >5% of the mean, much larger than the RMS values in figures 12 and 13.

*Liquid velocities close to the bubble interfaces*

Detailed examination of the velocity time series in conjunction with the probe data (LDA/EP technique) reveals the velocity of the liquid immediately before and after an individual passage, as shown in figures 15 and 16. Note that the eddies in the wake are detected in the liquid velocities trailing the bubbles.

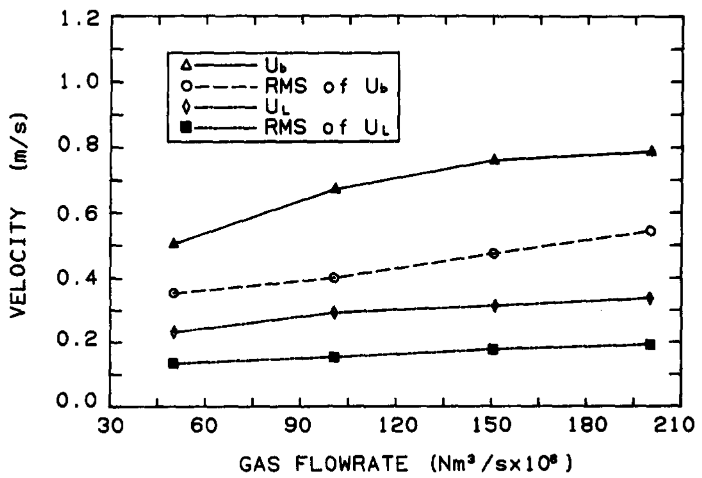


Figure 14. Bubble and liquid velocities in a bubbly plume determined with the combined LDA/EP technique. Large bubbles (5–40 mm) were produced by a flush-mounted orifice (4 mm dia) at the centre of the large model. The LDA was operated under the Combined/LDA mode with backward scattering. $U_b = 0.51$ to $0.79$ m/s, $\epsilon = 0.06$ to $0.12$ and $f_b = 2.8$ to $6.1$/s.

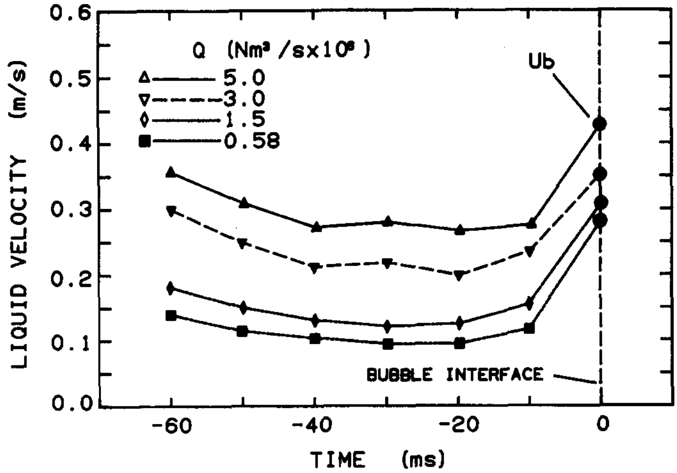


Figure 15. Liquid velocity variation before bubbles in a bubble chain using the combined LDA/EP technique. The chain was produced in the small model with an injection nozzle of 4 mm dia. The LDA was operated under the Combined/LDA mode with backward scattering. The circled points represent bubble velocities. $U_b = 0.28$ to $0.40$ m/s, $\epsilon = 0.09$ to $0.31$, $f_b = 6.5$ to $14.5$/s and $D_b = 5.43$ to $8.8$ mm.

## DISCUSSION

### *Discrimination by mixture PDF*

In figure 12, the gas and liquid velocities ± RMS are $0.05 \pm 0.006$ and $0.034 \pm 0.008$ m/s, respectively; and in figure 13 the corresponding values are $0.058 \pm 0.01$ and $0.048 \pm 0.018$ m/s, respectively. As the means become closer, and the RMS values increase, the distributions overlap. There are two major limitations of this technique when the distributions overlap:

(1) The observed mixture distribution becomes more of a straight line (more normal), making separation more difficult; one is not certain that data at the tails are due to either gas or liquid alone.
(2) The assumption that the individual gas and liquid distributions are normal and independent is not justifiable.

According to the present experimental results, it is not recommended to apply this technique to irregularly-shaped bubbles (> 15 mm) and void fractions > 0.4. This, of course, is only a general

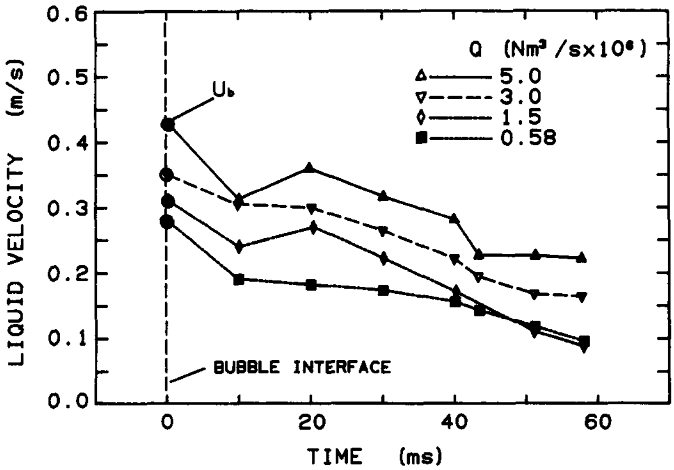


Figure 16. Liquid velocity variation following bubbles in a bubble chain using the combined LDA/EP technique. Note that eddies in the bubble wakes are detected. The conditions were the same as in figure 15. The circled points represent bubble velocities.

guideline because the useful upper limit will depend on the accuracy required, the distribution of bubble size and the level of turbulence.

*Discrimination by the LDA/EP technique*

This technique yields time series for gas and liquid velocities at a particular point, therefore it is useful for correlating these mean and RMS components. Other potential applications would include the measurement of drag coefficients, and the measurement of mass transfer coefficients as a function of interfacial fluctuations.

There are several variables which affect the quality of data which are discussed in the following sections.

*LDA configuration.* Forward scattering is not recommended for the measurement of bubble velocity because bubbles are larger than the control volume, and because the forward-scattered light may be intercepted by another bubble. Very good signals can be obtained from the bubbles in the back-scattering mode, however the liquid signals are relatively weak, resulting in a low data rate. This problem is largely alleviated by adjusting the seeding correctly so that the data rate for the back-scattered radiation from bubbles and liquid is comparable. Another possible solution to the problem is to measure the bubbles by back scattering and the liquid by forward scattering using two PMTs.

*EP position.* Several different positions for the EP relative to the control volume were evaluated; the best was $<1$ mm below the control volume. The time-scale resolution of this technique is of the order of the probe/LDA control volume separation divided by the bubble velocity. For the present experiments the separation was $<1$ mm, which makes the time resolution approx. 2 ms. The EP voltage reading is enabled by the LDA data-ready signal. When the EP signal is from a bubble, the LDA data will also be from the bubbles, most of the time. The exceptions are the instances in which the bubble interface is between the EP and the control volume. The fraction of incorrectly attributed velocities will be of the order of the ratio of the EP/control volume separation distance to the bubble height, which was always $<0.1$ and decreased to 0.01 for the larger bubbles.

*Limitations of the technique.* While the combined LDA/EP technique has been shown to be suitable for large bubbles at large void fractions, it is difficult to apply it to small bubbles at low void fraction because there are so few bubble signals compared to the liquid signals, and because small bubbles do not produce as large a change in EP response. Thus, the LDA/EP and PDF discrimination techniques are complementary.

Another shortcoming of the combined technique is that it is intrusive.

## CONCLUSIONS

1. Techniques to discriminate between gas and liquid signals based on laser signal waveform analysis or blockage of laser light are difficult to apply to large bubbles at moderate void fractions.
2. For small bubbles ($\leqslant 4$ mm) and small void fractions ($\leqslant 0.4$), the mean and RMS values for the gas and liquid velocities can be determined from manipulation of the combined velocity probability distribution function. The limits of applicability depend on the accuracy required, the uniformity of the bubble size and level of turbulence.
3. For larger void fractions and larger bubbles, a combined LDA/EP technique was developed for the simultaneous measurement of the bubble and liquid velocities inside a bubbly two-phase flow. The technique can also be used to measure the void fraction and bubble frequency.

*Acknowledgements*—The kind cooperation of Dr P. E. Wood during the experiments, which were carried out in his laboratory, is greatly appreciated. Financial support by the Canadian International Development Agency and the Natural Sciences and Engineering Research Council is gratefully acknowledged.

## REFERENCES


BANERJEE, S. & LAHEY, R. T. JR 1981 Advances in two-phase flow instrumentation. In *Advances in Nuclear Science and Technology*, Vol. 13 (Edited by LEWINS, J. & BECKER, M.), pp. 227–414. Plenum Press, London.

BOERNER, T., MARTIN, W. W. & LEUTHEUSSER, H. J. 1984 Comprehensive measurements in bubbly two-phase flows using laser-Doppler and hot-film velocimeter. *Chem. Engng Commun.* **28,** 29–43.

CASTILLEJOS, A. H. & BRIMACOMBE, J. K. 1987a Measurement of physical characteristics of bubbles in gas–liquid plumes: Part I. An improved electroresistivity probe technique. *Metall. Trans.* **18B,** 649–658.

CASTILLEJOS, A. H. & BRIMACOMBE, J. K. 1987b Measurement of physical characteristics of bubbles in gas–liquid plumes: Part II. Local properties of turbulent air–water plumes in vertically injected jets. *Metall. Trans.* **18B,** 659–671.

DRAIN, L. E. 1980 *The Laser Doppler Technique.* Wiley, New York.

DURST, F. & ZARE, M. 1975 Laser Doppler measurements in two-phase flows. *Proc. of the LDA Symp.* Copenhagen, pp. 403–429.

DURST, F., SCHNONUNG, B., SELANGER, K. & WINTER, M. 1986 Bubble driven liquid flows. *J. Fluid Mech.* **170,** 53–82.

HARDY, J. E. & HYLTON, J. O. 1984 Electric impedance string probes for two-phase void and velocity measurement. *Int. J. Multiphase Flow* **10,** 541–546.

HINZE, J. O. 1975 *Turbulence*, 2nd edn. McGraw-Hill, New York.

IRONS, G. A. & GUTHRIE, R. I. L. 1981 Bubbling behaviour in molten metals. *Can. Metall. Q.* **19,** 381–387.

LEE, S. L. & CHO, S. K. 1983 Simultaneous measurements of size and two velocity components of large droplets in two-phase flow by laser Doppler anemometry. In *Measuring Techniques in Gas–Liquid Two Phase Flow* (Edited by DELHAYE, J. M. & COGNET, G.), pp. 149–164. Springer, New York.

LEE, S. L. & DURST, F. 1982 On the motion of particles in turbulent duct flows. *Int. J. Multiphase Flow* **8,** 125–146.

LEE, S. L. & SRINIVASAN, J. 1978 Measurement of local size and velocity probability density distributions in two-phase suspension flows by laser-Doppler technique. *Int. J. Multiphase Flow* **4,** 141–155.

LEE, S. L. & SRINIVASAN, J. 1982 An LDA technique for *in situ* simultaneous velocity and size measurement of large spherical particles in two-phase suspension flow. *Int. J. Multiphase Flow* **8,** 47–57.

MARIE, J. L. & LANCE, M. 1983 Turbulence measurements in two-phase bubbly flows using laser Doppler anemometry. In *Measuring Techniques in Gas–Liquid Two Phase Flow* (Edited by DELHAYE, J. M. & COGNET, G.), pp. 141–148. Springer, New York.

MARTIN, W. W., ABDELMESSIH, A. H., LISKA, J. J. & DURST, F. 1981 Characteristics of laser-Doppler signals from bubbles. *Int. J. Multiphase Flow* **7,** 439–460.

MOMII, K., JINNO, K., UEDA, T. & HARADA, 1986 Study on LDA measurements and turbulence properties in solid–liquid two-phase flow. *Fluid Control Measur.* **2,** 807–812.

OHBA, K., KISHIMOTO, I. & OGASAWARA, M. 1976a Simultaneous measurements of local liquid velocity and void fraction in bubbly flows with a gas laser—Part I. Principle and measuring procedure. *Technol. Rep. Osaka Univ.* **26**(1328), 547–556.

OHBA, K., KISHIMOTO, I. & OGASAWARA, M. 1976b Simultaneous measurements of local liquid velocity and void fraction in bubbly flows with a gas laser—Part II. Local properties of turbulent bubbly flow. *Technol. Rep. Osaka Univ.* **27**(1358), 230–238.

OHBA, K., YUHARA, T. & MATSUYAMA, H. 1986 Simultaneous measurements of bubble and liquid velocities in two-phase bubbly flow using LDA. *Bull. JSME* **29**(254), 2487–2493.

SERIZAWA, A., KATAOKA, I. & MICHIYOSHI, I. 1975a Turbulent structure of air–water bubbly flow—I. Measuring techniques. *Int. J. Multiphase Flow* **2,** 221–233.

SERIZAWA, A., KATAOKA, I. & MICHIYOSHI, I. 1975b Turbulent structure of air–water bubbly flow—II. Transport properties. *Int. J. Multiphase Flow* **2,** 235–246.

SERIZAWA, A., KATAOKA, I. & MICHIYOSHI, I. 1975c Turbulent structure of air–water bubbly flow—III. Transport properties. *Int. J. Multiphase Flow* **2,** 247–259.

TROPEA, C. & STRUTHERS, D. 1987 Microprocessor based on-line measurement system for LDA. Presented at Deutsche-Franzosisches Forschungsinstitute, Saint-Louis, U.S.A.

TSUJI, Y. & MORIKAWA, Y. 1982 LDV measurement of an air–solid two-phase flow in a horizontal pipe. *J. Fluid Mech.* **120,** 385–409.

TSUJI, Y., MORIKAWA, Y. & SHIOMI, H. 1984 LDA measurement of an air–solid two-phase flow in a vertical pipe. *J. Fluid Mech.* **139,** 417–434.

UEDA, T., JINNO, K., MOMII, K. & NAKAJIMA, Y. 1986 Experimental study on turbulence in solid–liquid two-phase flow with Laser Doppler Anemometer. *Technol. Rep. Kyushu Univ. (Japan)* **59,** 787–792.

ZHAO, Y.-F. & IRONS, G. A. 1989 The breakup of bubbles into jets during submerged gas injection. *Metall. Trans.* **21B,** 997–1003.